# Mutual symbiosis of electroactive bacteria and denitrifiers for improved refractory carbon utilization and nitrate reduction

Yang, Xiangyu; Yao, Mingchen; Li, Peng; van der Hoek, Jan Peter; Zhang, Lujing; Liu, Gang

**Important note**
To cite this publication, please use the final published version (if applicable).
Please check the document version above.

Full length article

# Mutual symbiosis of electroactive bacteria and denitrifiers for improved refractory carbon utilization and nitrate reduction

Xiangyu Yang [a,b,c,d], Mingchen Yao [a,d,e], Peng Li [f], Jan Peter van der Hoek [d,g], Lujing Zhang [d,f], Gang Liu [a,d,e,*]

[a] Key Laboratory of Drinking Water Science and Technology, Research Centre for Eco-Environmental Sciences, Chinese Academy of Sciences 100085 Beijing, PR China
[b] Shandong Provincial Key Laboratory of Marine Environment and Geological Engineering (MEGE), College of Environmental Science and Engineering, Ocean University of China, 238 Songling Road, Qingdao 266100 PR China
[c] Key Laboratory of Marine Environment and Ecology, Ministry of Education, College of Environmental Science and Engineering, Ocean University of China, Qingdao 266100 PR China
[d] Section of Sanitary Engineering, Department of Water Management, Faculty of Civil Engineering and Geosciences, Delft University of Technology 2628 CN Delft, the Netherlands
[e] University of Chinese Academy of Sciences 100049 Beijing, PR China
[f] China Water Environment Group, Beijing 101101 PR China
[g] Waternet, Department Research & Innovation 1090 GJ Amsterdam, the Netherlands

## ARTICLE INFO

## ABSTRACT

Mutual symbiosis of electroactive bacteria (EAB) and denitrifier may be the key for solving the refractory carbon and residual nitrogen in wastewater treatment plant effluent. However, its application is hampered by unclear co-metabolic model and uncertain electron transfer. Here, we achieved 3–5 times increase in refractory carbon degradation, 40 % improvement in denitrification, and 36.0 % decrease in $N_2O$ emission by co-culturing *P. aeruginosa* strain GWP-1 and *G. sulfurreducens*. Such an enhancement is obtained by both refractory carbon co-metabolism and interspecies electron transfer (IET) between GWP-1 and *G. sulfurreducens*. Importantly, IET was quantified via isotopic approach, which revealed that *G. sulfurreducens* supplies more electrons to GWP-1 when the system was fed with cellulose (0.071 mM) than glucose (0.012 mM). This study demonstrates that the residual refractory carbon and nitrogen in treated wastewater could be further converted by mutual symbiosis of EAB and denitrifiers, which paves a synergic way for pollution and carbon reduction.

## 1. Introduction

As estimated, global wastewater production is about $359.4 \times 10^9$ $m^3$/year, of which 52 % is treated targeting on organic carbon and nitrogen removal (Jones et al., 2021). However, the current wastewater treatment is still considered a hotspot of environmental pollution and carbon emission (Rothausen and Conway, 2011; Wastewater monitoring comes of age, 2022). As reported, the wastewater treatment in EU, US, and China emitted 23 million, 45 million, and 53 million tons of $CO_2$-eq in 2019, respectively (Du et al., 2023). This is mainly due to the high energy and material consumption in wastewater treatment plants (WWTPs) (Wastewater monitoring comes of age, 2022). Besides, the considerable amounts of residual nitrogen (nitrate or nitrite) and carbon (e.g. cellulose) in effluents that are difficult to be removed by current biochemical processes (Zhou et al., 2022; Buzzini et al., 2006). For

example, Amsterdam's urban wastewater annually released 17,000–21,000 tons of cellulose, representing 25–30 % of the total COD load (van der Hoek et al., 2016), and these refractory carbon sources were discharged with effluents into the receiving water indirectly. In addition, WWTPs also discharge residual nitrogen when carbon sources for denitrification are missing (Garrido-Amador et al., 2023). Therefore, elevating the denitrification efficiency by utilizing refractory carbon sources (e.g. cellulose) in effluent would be ideal solution tackling carbon and nitrogen problems.

The integration of electroactive bacteria (EAB) and denitrifiers has been considered as a promising approach for sustainable wastewater treatment (Wan et al., 2018; Guo et al., 2023; Shi et al., 2016). Although significant progresses have been made regarding its performance on nitrogen removal and electricity generation, its wider application is hampered by the limited understanding on the co-metabolic pathways

and efficiency of interspecies electron transfer (IET) in such co-culture system (Graf et al., 2021). Studies have found significant amounts of EAB in wastewater treatment system, e.g., *Geobacter* was estimated to constitute approximately 10 %-14 % of the overall microbial community (Doherty et al., 2015; Aguirre-Sierra et al., 2020; Lu et al., 2015), and its abundance appeared to be positively correlated with the efficiency of nitrogen removal (Yan et al., 2021). However, most of EAB are generally unable to directly degrade refractory carbon sources (e.g. cellulose, lignin, hemicellulose, etc.), and on the contrary, *Geobacter* can absorb and metabolize small organic molecules produced by denitrifiers that degrade high-molecular carbon sources (Liu et al., 2017). Moreover, Wan, et al. (2018) have demonstrated an improvement of nearly 50 % in denitrification efficiency by introducing *G. sulfurreducens* into actual anaerobic denitrifying sludge with a low carbon-to-nitrogen ratio, which confirmed that *G. sulfurreducens* selectively enhanced the expression of the *nir*S gene coding for the nitrite reductase and leading to faster and more thorough denitrification. Although it is established that EAB can promote denitrifiers in completing the nitrogen removal process, several scientific questions about the internal mechanisms of this process remain unresolved. These include: i) Whether EAB and denitrifiers can co-metabolize carbon sources, especially refractory carbon sources like cellulose; ii) How the co-metabolic model of EAB and denitrifiers responds to receiving and giving electrons; iii) How to determine the electron transfer path and quantify the transferred electrons of each transfer path.

To answer these questions, further studies employing binary culture systems are needed to determine the mechanisms underlying the mutual symbiosis between EAB and denitrifiers. In this study, the denitrification efficiency of *P. aeruginosa* GWP-1 (sieved from denitrifying sludge) and *G. sulfurreducens* co-cultured system was investigated with glucose and cellulose as carbon sources. The key protein enzymes and electron transfer quantity were qualitatively and quantitatively investigated. Integrally, the emitted nitrous oxide ($N_2O$) was monitored together with carbon degradation and nitrogen removal. Overall, this study is expected to unveil co-metabolic pathway and IET between EAB and denitrifiers and also to hold broader significance for achieving rapid enhancement and stable operation of denitrifiers in wastewater treatment systems with refractory carbon sources.

## 2. Materials and methods

### 2.1. Preparation of strains and synthetic wastewater

*Geobacter* (*G.*) *sulfurreducens* PCA (ATCC-51573) was activated from laboratory frozen stocks, and *Pseudomonas* (*P.*) *aeruginosa* strain (named GWP-1, GenBank: OR143777.1) was enriched and screened for the first time in our study. For the GWP-1 isolation, the enrichment was initiated with a secondary sedimentation tank sample, in which the relative abundances of denitrifiers (represented by *nir*S number/16S rRNA gene) were 18.6 %. The highest dilution denitrification was transferred into the liquid medium amended with 2.0 % agar with vitamin solution (1 mL·L$^{-1}$) and appropriate electron donor and acceptor (10 mM sodium cellulose and 20 mM sodium nitrate) (Wang and He, 2020). The pH of the liquid medium was kept constant at 7.0 before the experiment. The enrichment medium for GWP-1 isolation was modified with a $N_2/CO_2$ [80:20 (vol/vol)] atmosphere at 30 °C under sterilizing oxygen-free stocks. Colonies were visible after five days. Individual colonies were picked with a disposable, sterilized needle in an anaerobic chamber and transferred into the streak plate containing 10 mL solid medium. This process was completed six times to further purify and achieve the homogeneity and single GWP-1 colony (Huang et al., 2022). To identify the strain, a near full-length 16 S rRNA gene sequence was PCR amplified using the universal primer 27F(5′-AGAGTTTGATCCTGGCTCAG-3′) and 1490R(5′-TACGGCTACCTTGTTACGACTT-3′). The 16S rRNA gene amplicon sequence was deposited in the National Center for Biotechnology Information (NCBI) database and annotated using NCBI's online

Basic Local Alignment Search Tool (BLAST). Fig. S1 depicts GWP-1′s phylogenetic relationship and functions compared to other species within the same genus of *Pseudomonas*. GWP-1 is closely related to *P. aeruginosa* ATCC 15692 and PAO1, both of which are capable of denitrification and cellulose degradation.

In experiment, the 100 μL of pure GWP-1 and *G. sulfurreducens* were inoculated into the liquid pressure-resistant sterile flasks. The culture medium was prepared by simulating the composition of bio-tank effluent (Text S1), and the composition was approximately 90 mg COD /L from glucose and cellulose and 15 mg/L $NO_3^-$-$^{15}$N from $K^{15}NO_3$ ($^{15}$N for the calculation of electron transferring capacity) according to pervious study with slight modification (Chen et al., 2015). The initial pH of the culture medium was adjusted to 7.0. The anthraquinone-2,6-disulfonate (AQDS) as the efficient electron mediators was added into the culture medium to enhance the IET process at a concentration of 100 μg/L. Before inoculating bacteria, the culture medium was treated at the high temperature (121 °C) and helium (He) blowing (10 min) to ensure the sterility and anoxic conditions.

### 2.2. Experimental design and procedures

The experiment was divided into two treatments: control group (glucose as "simple" carbon source, "S") and treatment group (cellulose as "hard" carbon source, "H"). According to the presence or absence of AQDS, each group was set into two batches: no AQDS (control, CK) and AQDS (enhanced, E), and each batch was set into three groups: CK/CKE (no microorganisms with/without AQDS), P/PE (only GWP-1 with/without AQDS), GP/GPE (co-existence of *G. sulfurreducens* and GWP-1 with/without AQDS). All experimental groups were set in absolute anaerobic conditions in triple treatments. Therefore, in the experiment there are 36 microcosm systems (Fig. S2). The culture medium was placed in a 250 mL pressure-resistant sterile flask (liquid/headspace ratio is 3/2), and the OD$_{600}$ value of culture medium with bacteria solution was within the range of 0.7–0.72. After inoculation and sealing, the flask was placed in an air bath incubator with 100 rpm and at 30 °C constant temperature for culture, and the whole process was carried out in an anaerobic glove box before sealing.

### 2.3. Solution and gas detection

Solution samples were taken from each flask at 0, 2, 4, 8, 12, 18, 24, 36, 48, 56, 64, 72, 80, 88, 96, 108, and 120 h by a 2 mL syringe. The water samples were filtered through 0.22 μm polyethersulfone filters and immediately stored at −20 °C until analysis, and then the water qualities were analyzed after diluting by using the segmented flow analyzer (SAN++, SKALAR, Netherlands). After the 5-days experiment, the headspace gas samples were undertaken by a syringe driving by the inter-pressure and stored in the 10 mL gas bag. The gas samples were measured using gas chromatography with the ECD (for $N_2O$) detectors (GC-2010Plus, Shimadzu, Japan) (Su et al., 2021).

The $N_2O$ emission equivalent was calculated by the following equation:

$$N_2O \text{ emission equivalent}(mMCO_2) = 273 \times V \cdot C_{N_2O} \qquad (1)$$

where $C_{N2O}$ and V is the $N_2O$ concentration (mM) and volume (ml), respectively; and "273" is constants for transforming $N_2O$ into $CO_2$-equivalent emissions (Climate Change, 2022).

### 2.4. Characterization of AQDS electrochemical property

**Electron spin resonance (ESR) measurements:** This approach has previously been used as an indicator for the quinone and hydroquinone (AHAQDS and AH$_2$AQDS) content in AQDS solution (Scott et al., 1998). The ESR spectra were obtained with a ESP300E spectrometer (Bruker, Germany). With the ESR measurements, the liquid culture medium was

added with a 0.1 M NaOH solution to obtain a 10 % v/v concentration. A glass capillary was then immediately filled with the solution and placed into the ESR cavity. The concentration of organic radicals was measured as a function of time in the basic solution at room temperature to obtain a stable concentration of organic radicals. The ESR instrument was operated with the following parameters: microwave frequency 9.85 GHz, microwave power 20 mW, modulation frequency 100 kHz, conversion time 16 ms, and time constant 81.92 ms. Signal intensity varied linearly with the square root of the microwave power ($R^2 = 0.9997$), indicating that power saturation was avoided under the operating conditions of the instrument. 3-Carbamoyl-2,2,5,5-tetramethyl-3-pyrrolin-1-yloxy, a compound containing a nitroxyl free radical, was used as the standard for ESR. The spectra were electronically integrated on the Bruker ESP300E instrument. Replicate samples (n = 3) were measured to determine standard deviations. After the data file was exported, the Origin software was used for processing and drawing.

**Electron-accepting (EAC) and electron-donor (EDC) capacities:** Electrochemical experiments were performed with an electrochemistry workstation (CHI660D, Chenhua Co. Ltd, China) with a conventional three-electrode cell at an ambient temperature (Guo et al., 2023). A platinum plate electrode (Pt) with a projected surface area of 5 $cm^2$ was used as the working electrode, and Pt net and Ag/AgCl electrodes as the counter and reference electrodes, respectively. The chronoamperometry (CA) measurements were performed to evaluate the EDC and EAC of AQDS or AHQDS in a $N_2$ saturated PBS (pH = 7.2) at a potential of $-0.6$ V (vs. Ag/AgCl) under stirring. Chronoamperometric curves of AQDS in culture solution containing bacteria cells were detected at the applied potentials of $-1.0$ V and $+1.0$ V at the begin and end of the experiment, respectively (Yuan et al., 2011). After the data file was exported, the Origin software was used for processing and drawing. Detailed, the quantification method primarily involves scanning the electron capacity of the culture system over a unit time using an electrochemical workstation. The scanning results are analyzed using Origin software to integrate the peak area, which reflects the electron acquisition and loss capacity of AQDS.

### 2.5. Characterization of microbial morphology

After the formal experiment, 5 mL of culture medium were sampled from each microcosm flask to use for observing microbial morphology and the co-existence relationship of EAB (rhabditiform) and denitrifiers (sphericity) under the scanning electron microscope (SEM, Quattro S, Thermo Fisher, U.S.) (Liu et al., 2019; Liu et al., 2012). The procedure of SEM was as follows: culture medium containing EAB and denitrifiers were centrifuged with a 5 mL centrifuge tube at 8000 rpm, 4 °C for 5 min and were washed three times with the phosphate buffer (0.1 M, pH = 7.4). Then, 2.5 % glutaraldehyde was added to fix the bacteria at 4 °C for at least 4 h. Subsequently, the bacterial samples were dehydrated in ethanol and tertiary butanol serials (50 %, 70 %, 80 %, 90 %, and 100 %, 15 min per step). Finally, the dehydrated bacterial samples were dried using a critical evaporator. The dried bacterial samples were mounted on aluminum stubs, coated with gold, and imaged using the SEM.

Fluorescence in situ hybridization (FISH) analysis was referenced to previous study (Roots et al., 2019). Oligonucleotide probes for FISH were designed specifically for targeted bacteria cells with (EAB: 5′-GAAGACAGGAGGCCCGAAA-3′ labeled with CY5 and denitrifiers: 5′-GCTGGCCTAGCCTTC-3′ labeled with 6-FAM) and used for microscopic identification of the filamentous EAB and spherical denitrifiers by FISH. The plates were examined using the confocal laser scanning microscope (CLSM, Leica, TCS SP8 CSU, Germany). The detail profile is provided in the Supplementary Materials (Text S2).

### 2.5.1. Microbial growth monitoring

Solution samples were taken from each flask at 0, 10, 24, 48, 72, 96, and 120 h. All samples were maintained in an ice box as soon as possible and then analyzed within 24 h. Adenosine triphosphate (ATP)

measurements and quantitative PCR (qPCR) analysis were used to analyze the total bacteria activity and quantify the bacteria abundance and denitrifying function. The measurements of ATP and qPCR were conducted as described by Yao et al. (Yao et al., 2023) and Livak et al. (Livak and Schmittgen, 2001). Among, details of the DNA extraction for qPCR analysis were described in our previous publication (Yang et al., 2022; Yang et al., 2020), and the information of primers are listed in the Supplementary Materials (Table S1). The detail processes are described in Supplementary Materials (Text S3).

### 2.5.2. Proteomic analysis

At the end of 120 h experiment, the bacteria suspensions in a part of experiment groups (P, GP, and GPE) with feeding glucose or cellulose were collected and centrifuged at 8000 g under 4 °C for 10 min to obtain the bacterial precipitates. And then, the bacterial precipitates were sent to the Majorbio Bio-Pharm Technology Co., Ltd. (Shanghai, China) for proteomic analysis. The detail processes are described in Supplementary Materials (Text S4). Finally, based on the quantitative results, the function enrichment analysis, protein–protein interaction (PPI) and subcellular localization analysis of the differential proteins were performed (Ma et al., 2020; Xu et al., 2019; Zhu et al., 2020). The mass spectrometry proteomics data have been deposited to the ProteomeXchange Consortium (https://proteo-mecentral.proteomexchange.org) via the iProX partner repository (Ma et al., 2019) with the dataset identifier PXD044018. In this study, the key proteins with the remarkable fluctuation of abundance in main metabolic pathways in different culture systems was analyzed. For GWP-1, the relative abundance of HGP vs. HP and HGPE vs. HGP was compared, and for *G. sulfurreduens*, HGPE vs. HGP and HGP vs. SGP were compared. In addition, 'Rich Factor' was calculated to indicate the degree of differentially expressed proteins in different groups.

### 2.5.3. Electron-transferring efficiency

Electron transfer efficiency was measured in this study through an electron respiration approach by reducing tetrazolium chloride to formazan (Yang et al., 2020; Broberg, 1985). After the 120 h experiment, 5 mL of bacterial solution were collected from each bottle in all groups and placed in a 50 mL centrifugal tube. Bacterial solution was first washed with 4 °C 0.05 M PBS thrice. 5 mL 0.5 % tetrazolium chloride and 5 mg NADH were added into the centrifugal tube. After incubation in the dark for 30 min (25 °C), 1 mL formaldehyde (HCHO) was injected into the centrifugal tube to terminate the reaction. The supernatant of the mixture was removed by centrifuging at 4500 rpm for 10 min. Then, 5 mL 96 % methanol was added into the treatment samples, and the centrifugal tube was shaken to extract formazan at 200 rpm for 30 min. The supernatant was collected after being centrifuged at 8,000 rpm for 5 min. Absorbance of the generated orange-like supernatant was quantified at 490 nm. The electron transfer efficiency was estimated as following:

$$ETE(\mu gO \cdot min^{-1} \cdot ml^{-1} solution) = \frac{ABS_{490}}{15.9} \cdot \frac{V}{V_0 t} \cdot 16 \cdot \frac{1}{V_m} \quad (2)$$
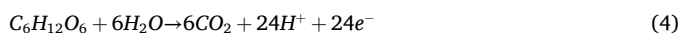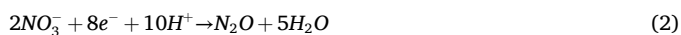
where $ABS_{490}$ is the absorbance of the supernatant at 490 nm; 15.9 is the absorptivity of tetrazolium chloride − formazan; $V_0$ and V (ml) are the volumes of initial mixture and methanol, respectively; t (min) is the incubation time; 16 is the factor for the transformation of tetrazolium chloride–formazan to O; and $V_m$ (item) is the column of bacteria solution.

### 2.5.4. Electron-transferring capacity
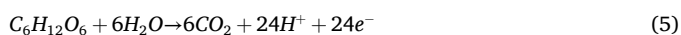
After the experiment, the volume of the upper space of the culture bottle was recorded, and $^{15}NO$, $^{15}N_2O$, $^{15}N_2$ and $CO_2$ gases were collected for concentration detection, and the yield of each component was calculated. Isotopic ratio mass spectrometer was used to detect the proportion of isotopically labeled elements in each component and to

calculate the content of isotopically labeled gas components in each component (Niemann et al., 2005). Finally, according to the law of material balance and conservation of electrons, the efficiency and improvement of denitrification and nitrogen removal driven by EAB were calculated. The detailed calculation process is as follows:

- For GWP-1 (shorted by P.):

$$NO_3^- + 3e^- + 4H^+ \rightarrow NO + 2H_2O \tag{1}$$

$$2NO_3^- + 8e^- + 10H^+ \rightarrow N_2O + 5H_2O \tag{2}$$

$$2NO_3^- + 10e^- + 12H^+ \rightarrow N_2 + 6H_2O \tag{3}$$

$$C_6H_{12}O_6 + 6H_2O \rightarrow 6CO_2 + 24H^+ + 24e^- \tag{4}$$

- For *G. sulfurreducens* (shorted by G.):

$$C_6H_{12}O_6 + 6H_2O \rightarrow 6CO_2 + 24H^+ + 24e^- \tag{5}$$

First of all, in the denitrification process, $NO_3^-$-N was reduced to produce NO (formula (1)), $N_2O$ (formula (2)) and $N_2$ (formula (3)), which required the total of **N** e⁻, namely:

$$\sum e_{P.}^- = \sum e_{NO}^- + \sum e_{N_2O}^- + \sum e_{N_2}^- = Ne^- \tag{6}$$

Second, in the whole culture system, the microbial respiration (GWP-1 and *G. sulfurreducens*) completely degraded glucose and cellulose to produce $CO_2$ (No other organic metabolite) (formula (4) and (5)), which could release **M** e⁻, namely:

$$\sum e_{CO_2}^- = \sum e_{P.CO_2}^- + \sum e_{G.CO_2}^- = Me^- \tag{7}$$

Among them, the number of electrons from denitrifiers degrading glucose through respiration was assumed to be **a** e⁻, the total number of electrons generated by respiration of *G. sulfurreducens* was assumed to be **b** e⁻, and the number of electrons provided by *G. sulfurreducens* to GWP-1 through IET was assumed to be **x** e⁻. **M, N, a, b,** and **x** have the following relationship:

$$ae^- + be^- = Me^- \tag{8}$$

$$ae^- + xe^- = Ne^- \tag{9}$$

By quantifying the headspace volume, M and N can be accurately obtained. As the presence/absence of AQDS had no effect on the physiological activity of denitrifiers, the electron contents (**a** e⁻) produced by denitrifiers degrading substrate were constant. When **a** was a constant value, in formula (8) and (9), $\Delta N = \Delta x$, $\Delta M = \Delta b$. In no AQDS groups, the total number of electrons transferring from *G. sulfurreducens* to GWP-1 was **x** e⁻, and the total number of electrons generated by *G. sulfurreducens* was **b** e⁻. In the AQDS groups, the abovementioned numbers were improved into $x+\Delta x$ and $b + \Delta x$. To compare the increase of electron content transferring from *G. sulfurreducens* to GWP-1 in glucose and cellulose groups, we first calculated the **x** value. Since in the same carbon source group, the presence/absence of AQDS only changed the efficiency of electron transfer but not the transfer capacity, the values of $\frac{x}{b}$ and $\frac{x+\Delta x}{b+\Delta x}$ should be equal ($\frac{x}{b} - \frac{x+\Delta x}{b+\Delta x} = 0$). Furthermore, the formula $\frac{x}{b} - \frac{x+\Delta x}{b+\Delta x}$ can be changed to $\frac{(\Delta M - \Delta N)x - \Delta N(b-x)}{b(b+\Delta M)}$, therefore $(\Delta M - \Delta N)x - \Delta N(b-x) = 0$. Assuming that $(\Delta M - \Delta N)x - \Delta N(b-x) = 0$, we can get $x = \frac{\Delta N(b-x)}{\Delta M - \Delta N}$. Formula (8)-(9) can get $b - x = M - N$. Therefore, $x = \frac{\Delta N(M-N)}{\Delta M - \Delta N}$ can be derived. At this point, the value of $^{15}NO$, $^{15}N_2O$, $^{15}N_2$ and $CO_2$ gases we detected through isotopic tracers were plugged into the final formula, and we could quantify and compare the number of electrons transferring from *G. sulfurreducens* to GWP-1 (**x** e⁻) in glucose and cellulose groups, respectively.

## 2.6. Statistical analysis

All data assays were conducted in triplicate, and the results are presented as mean ± standard deviation. Analysis of variance (ANOVA) was used to compare results by group; $p < 0.05$ was considered to be statistically significant (SPSS 22.0, IBM). In the proteinic analysis, 'Rich Factor' is calculated by dividing the number of differentially expressed proteins annotated to that pathway by the total number of identified proteins annotated to that pathway.

## 3. Results

### 3.1. Growth dynamics of GWP-1 and G. sulfurreducens

Using glucose as carbon source, the bacterial growth dynamics showed expected patterns for both pure and co-cultured systems (Fig. 1a and S3). Differently, using cellulose as carbon source, the growth of *G. sulfurreducens* was significantly inhibited, while the growth of GWP-1 was not influenced which showed similar, though lower, peaks in both pure and co-cultured systems compared to using glucose as carbon source (Fig. 1b). The above results indicate that *G. Sulfurreducens* can co-grow with GWP-1 via co-metabolizing the inedible carbon sources (only for *G. Sulfurreducens*), but it grew slowly in utilizing cellulose than glucose. Interestingly, the presence of AQDS greatly favored the growth of *G. sulfurreducens*, which is especially true for the case using cellulose, because *G. sulfurreducens* relied on AQDS for the electron transfer (Fig. 1b and S2b).

### 3.2. Denitrification performance

Using glucose as carbon source, nitrate removal remained consistently high (57.6 % ± 6.7 %) across all experimental groups, with negligible nitrite accumulation (0.060 ± 0.010 mg/L) (Fig. 2a). Differently, when using cellulose as carbon source, *G. sulfurreducens* significantly enhanced nitrate removal in the co-cultured systems (GP, 43.3 %) compared to the pure cultured system (P, 28.3 %; PE, 12.2 %). The addition of AQDS further increased nitrate removal to 64.6 % (GPE). In co-culture systems (GP and GPE), there was nitrite accumulation in the middle stage (50–60 h, ~ 0.20 mg/L), which may be due to the rapid reduction of nitrate to nitrite, but not enough electrons to further reduce. And then, the accumulating nitrite gradually decreased towards the end of the experiment. Additionally, the degradation ability of denitrifiers to cellulose was also improved in the co-culture system compared to the pure GWP-1 system (increasing 3.0 – 5.0 folds), and it was further enhanced by the presence of AQDS. This improvement even was basically similar to that of glucose carbon source (Fig. S4).

Regarding the $N_2O$ emission, as shown in Fig. 2b, the $N_2O$ emission equivalent ($CO_2$-eq) was lower in co-cultured systems than in pure GWP-1 systems, which was further reduced by adding AQDS. Remarkably, the presence of *G. sulfurreducens* and AQDS contributed to a significant reduction in $CO_2$-eq in the co-culture systems using both glucose and cellulose as carbon source. For co-cultured systems fed with cellulose (GPE), the addition of AQDS contributed to 17.8 % reduction in $CO_2$-eq compared to the co-cultured systems without AQDS and 36.3 % reduction compared to the pure culture system with only GWP-1. Overall, the integral analysis of water and gas samples demonstrated that the presence of EAB and AQDS not only increased the denitrification efficiency but also reduced $N_2O$ emission regardless fed with glucose or cellulose as carbon source. In order to explain these results, we conducted a verification analysis of the IET and substrate co-metabolism processes in the co-culture systems.

### 3.3. Interspecies electron transfer between GWP-1 and G. sulfurreducens

Fig. 3a shows that benzoquinone moieties were gradually reduced to semiquinone moieties as the main organic radicals over time, indicating
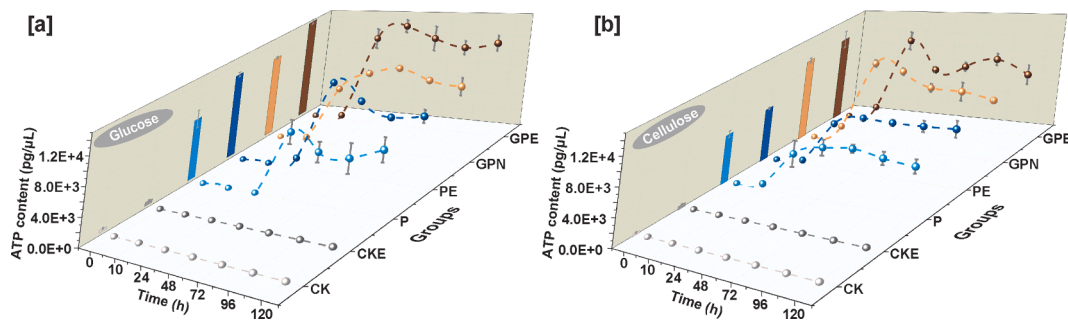
**Fig. 1.** The growth kinetics curve of *G. sulfurreducens* and *P. aeruginosa* strain GWP-1 in the different systems and temporal variations in the unique gene abundance ratio of the two bacteria in the co-cultured systems feeding with glucose [**a**] and cellulose [**b**]. Data are presented as the means ± standard deviation, n = 3.
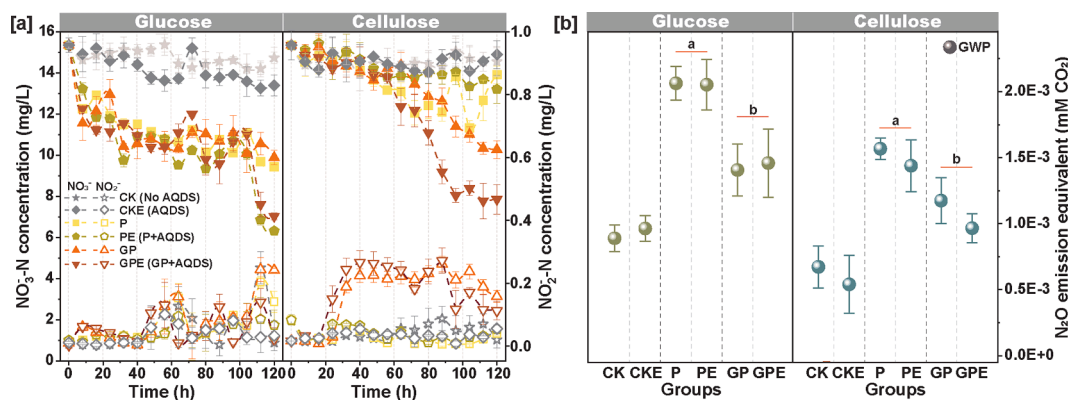


**Fig. 2.** [**a**] Temporal variations in $NO_3^-$-N and $NO_2^-$-N concentrations for 120 h feeding with glucose and cellulose in the presence/absence of AQDS in the different culture systems. [**b**] The $N_2O$ emission equivalent in the different culture systems after 120 h. The different letters (a and b) indicate statistically significant differences between the different culture systems. Data are presented as the means ± standard deviation, n = 3.

that AQDS received and stored electrons transferred from *G. sulfurreducens*. This is confirmed by results of electron acceptor capability (EAC) and electron donor capability (EDC) of AQDS (Fig. 3b-e). Initially, AQDS displayed strong EAC (840 µmol·e⁻/g) and weak EDC (3.9 µmol·e⁻/g), which reversed 120 h later (EDC, 220 µmol·e⁻/g; EAC, 6.72 µmol·e⁻/g). Notably, the fluctuating redox state of AQDS suggested its continuously gain and loss of electrons (Fig. 3c and 3e). These results provided direct evidence for the presence of an indirect IET process in the co-culture system facilitated by AQDS.

Besides, the FISH images revealed distinct clusters formed by the two species, with interweaving bacteria resembling the cluster form. Notably, the clusters were predominantly composed of *G. sulfurreducens* in the inner region and GWP-1 in the outer region (Fig. 3f). As depicted in Fig. 3g and 3 h, many thin pili structures were clearly observed by SEM images between *G. sulfurreducens* and GWP-1 in the co-cultured systems, which may be considered as potential evidence for possible existence of direct IET.

### 3.4. Quantifying interspecies electron transfer

According to formula 1–9, the average electron transport efficiency (ETE) in cellulose-fed co-cultured systems were 23.2 % lower than in those feds with glucose (Fig. 4). By adding AQDS, the ETE increased by 36.5 % in glucose-fed co-cultured systems, but no significant increase was observed in cellulose-fed co-cultured systems. Specifically, the number of electrons accepted for denitrification (N) in the cellulose-fed co-cultured systems was significantly lower than in the glucose-fed systems. The addition of AQDS promoted electron utilization for nitrate reduction for co-cultured systems fed with both glucose (ΔN = 0.0070 mM e⁻) and cellulose (ΔN = 0.0030 mM e⁻) (Fig. 4c). As mentioned above, these results align with the observed trends of

denitrification efficiency. Similarly, the generation of electrons through respiration (M) in the glucose-fed co-cultured systems was significantly higher than in those fed with cellulose, and the addition of AQDS enhanced the respiration process and electron generation (ΔM = 0.0090 mM e⁻, glucose; ΔM = 0.029 mM e⁻, cellulose; Fig. 4c). Hence, the difference between donor and acceptor electrons revealed significant differences in electron-storing potential (M−N) between co-culture systems fed with glucose (0.064–0.090 mM e⁻) and cellulose (0.021–0.024 mM e⁻), highlighting the importance of AQDS for electron-storing potential. The efflux electrons from extracellular electron acceptor bacteria (i.e., *G. Sulfurreducens*) are likely stored in AQDS as semiquinone groups. More specifically, *G. sulfurreducens* supplies more electrons to denitrifiers when fed with cellulose (x = 0.071 mM e⁻, $\bar{x}$=0.025 mM/mg·cellulose, with AQDS) compared to fed with glucose (x = 0.012 mM e⁻, $\bar{x}$=0.0030 mM/mg·cellulose, with AQDS). Overall, these results indicate that IET processes between EAB and denitrifiers collectively enhanced ETE in the co-cultured systems, especially under the enhancement of AQDS, and in cellulose group there was more electron transferring from EAB to denitrifier.

### 3.5. Co-metabolism processes between GWP-1 and G. sulfurreducens

Fig. 5 illustrates the statistical analysis of protein abundance changes. It revealed that the presence of *G. sulfurreducens* particularly increased the abundances of key protein enzymes in GWP-1 regarding carbon metabolism, electron and energy conversion, and denitrification (Fig. 5a). Meanwhile, the abundances of key protein enzymes in extracellular respiration of *G. sulfurreducens* were significantly higher in the cellulose group than in the glucose group, and the results was further increased by the presence of AQDS (*P* value < 0.05, Fig. 5a and 5b). Remarkably, the key enzymes responsible for cellulose degradation,
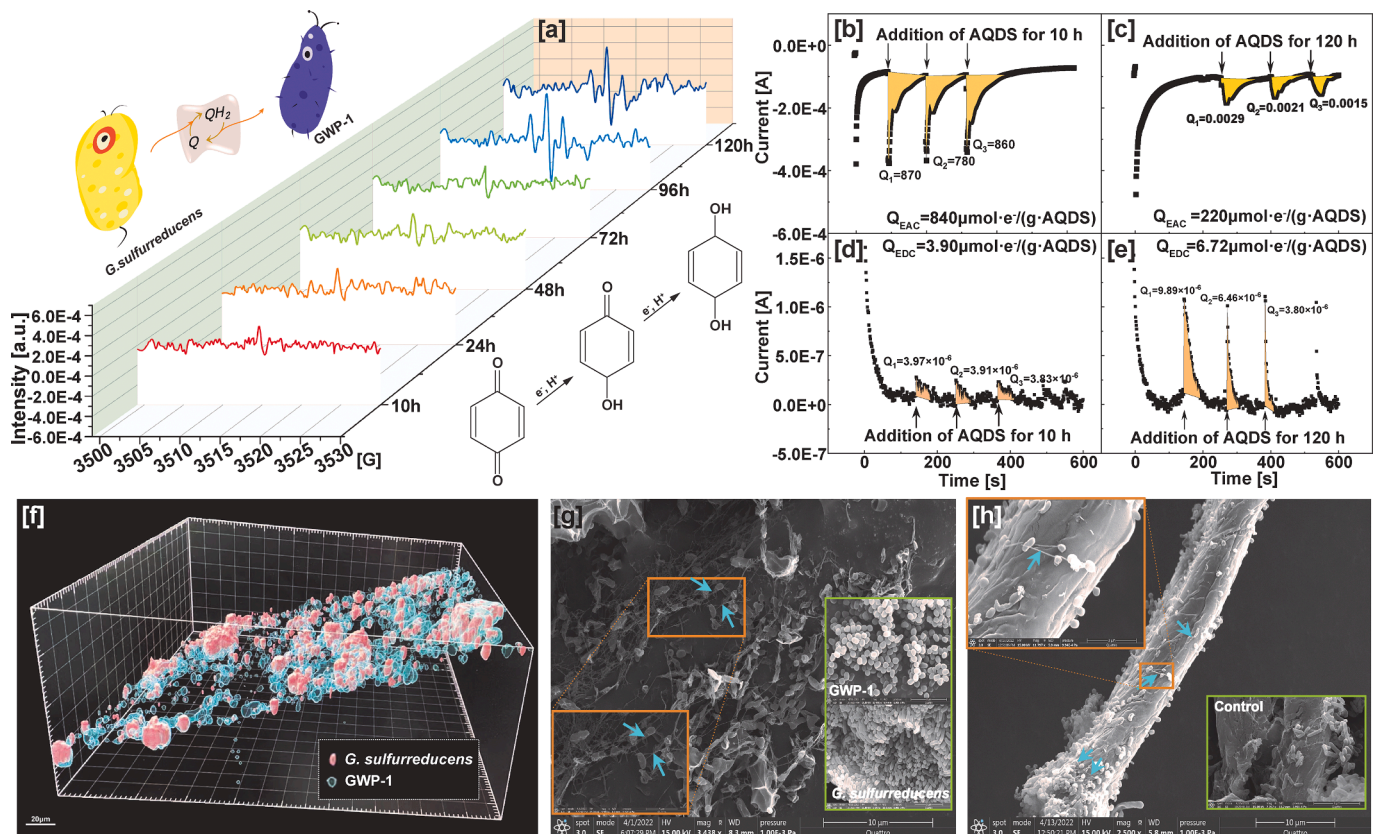
**Fig. 3.** The direct evidences of the interspecies electron transfer between *G. sulfurreduens* and GWP-1. **[a]** Variation of hydroquinone@AQDS (AHAQDS or AH₂AQDS) (in abscissa) using ESR spectra for the co-culture systems. The ESR instrument was measured using a gaussmeter probe and operated with the following parameters: microwave frequency 9.85 GHz, microwave power 20 mW, modulation frequency 100 kHz, conversion time 16 ms, and time constant 81.92 ms. The semiquinone species contains an unpaired electron could be measured. **[b-e]** Chronoamperometric curves of AQDS in culture solution at the applied potentials of −1.0 V (**[b]** for 0 h and **[c]** for 120 h) and +1.0 V (**[d]** for 0 h and **[e]** for 120 h) (vs. Ag/AgCl) at the begin and end of the experiment. The arrows indicate the addition of the co-culture strain solution with AQDS. **[f]** Scanning laser confocal microscopy image of the aggregates after FISH, which targeted *G. sulfurreduens* cells with a red probe (Cy3) and the GWP-1 cells with an indigo probe (Cy5). **[g-h]** SEM images for aggregates formed in colocalization of *G. sulfurreducens* (rhabditiform) and GWP-1 (sphericity) in 120 h after initiating the cultivation in the glucose **[g]** and cellulose **[h]**, and the pili structures (arrow pointing) were distinctly seen between the two strains in both the glucose and cellulose groups. (For interpretation of the references to colour in this figure legend, the reader is referred to the web version of this article.)

such as endoglycanase (2.67 folds) and β-glucosidase (3.72 folds), exhibited a significant increase in abundance in the co-cultured systems compared to pure culture systems. These results suggested carbon co-metabolism between the *G. sulfurreducens* and GWP-1, benefiting cellulose utilization and nitrate reduction (Fig. 5a). Moreover, the addition of AQDS further increased the relative abundance of key protein enzymes of carbon metabolism in *G. sulfurreducens* and GWP-1. The abundances of nitric oxide reductase (NOR) and nitrous oxide reductase (N₂OR) enzymes in GWP-1 were significantly higher by above 1.5 folds compared to systems without AQDS, which aligned with the observed trends of $NO_3^-$-N reduction and N₂O emission as shown in Fig. 2a and Fig. 2b. The abundances of NADH dehydrogenase and cytochrome proteins (MacA, PpcB, OmcB, OmcC, and OmcZ) in *G. sulfurreducens* were also significantly higher by 1.36–3.27 folds compared to systems without AQDS (Fig. 5). Overall, as confirmed by proteomics results, *G. sulfurreducens* was capable to utilize small molecule carbon produced from cellulose and glucose degraded by GWP-1. Moreover, through the IET process, electrons generated by extracellular respiration are transferred to GWP-1 and promoted carbon co-metabolism and denitrification efficiency.

## 4. Discussion

In previous studies, the mutual symbiosis processes involving EAB mainly focused on enhancing redox reactions that were otherwise difficult to achieve through IET. For instance, the co-culture of *G. sulfurreducens* and *G. metallireducens* not only enhanced ethanol degradation but also facilitated fumarate reduction, with the addition of granular activated carbon significantly accelerating this process (Liu et al., 2012; Summers et al., 2010). Similarly, the co-culture of *G. metallireducens* and *Methanosaeta* improved methane production from recalcitrant acetate, while the addition of conductive magnetite or activated carbon further enhanced methane yield (Morita et al., 2011; Kato et al., 2012). Additionally, the co-culture of *G. sulfurreducens* and *Thiobacillus denitrificans* utilized sodium acetate, a substrate that denitrifying bacteria cannot degrade, to reduce nitrate, which was significantly promoted by the addition of magnetite or $Fe^{3+}$ ions (Kato et al., 2012). These studies shared a common characteristic: the organic substrates are preferentially utilized by EAB, which transfer the electrons generated via electron mediators to other bacteria, enabling the reduction or degradation of other compounds. However, in practical wastewater treatment systems, most carbon sources are not readily utilized by EAB, i.e., glucose and cellulose. Moreover, there are limited studies on the co-metabolism of carbon sources and electron syntrophy between EAB and denitrifying bacteria. Particularly, research on substrates that can be directly utilized by denitrifying bacteria but are efficiently degraded by EAB through co-metabolism, with effective IET process, to enhance nitrate reduction from low-carbon effluent is rarely reported. The findings of our study provided a new insight from two perspectives: on one hand, it demonstrated that EAB could form microbial aggregates
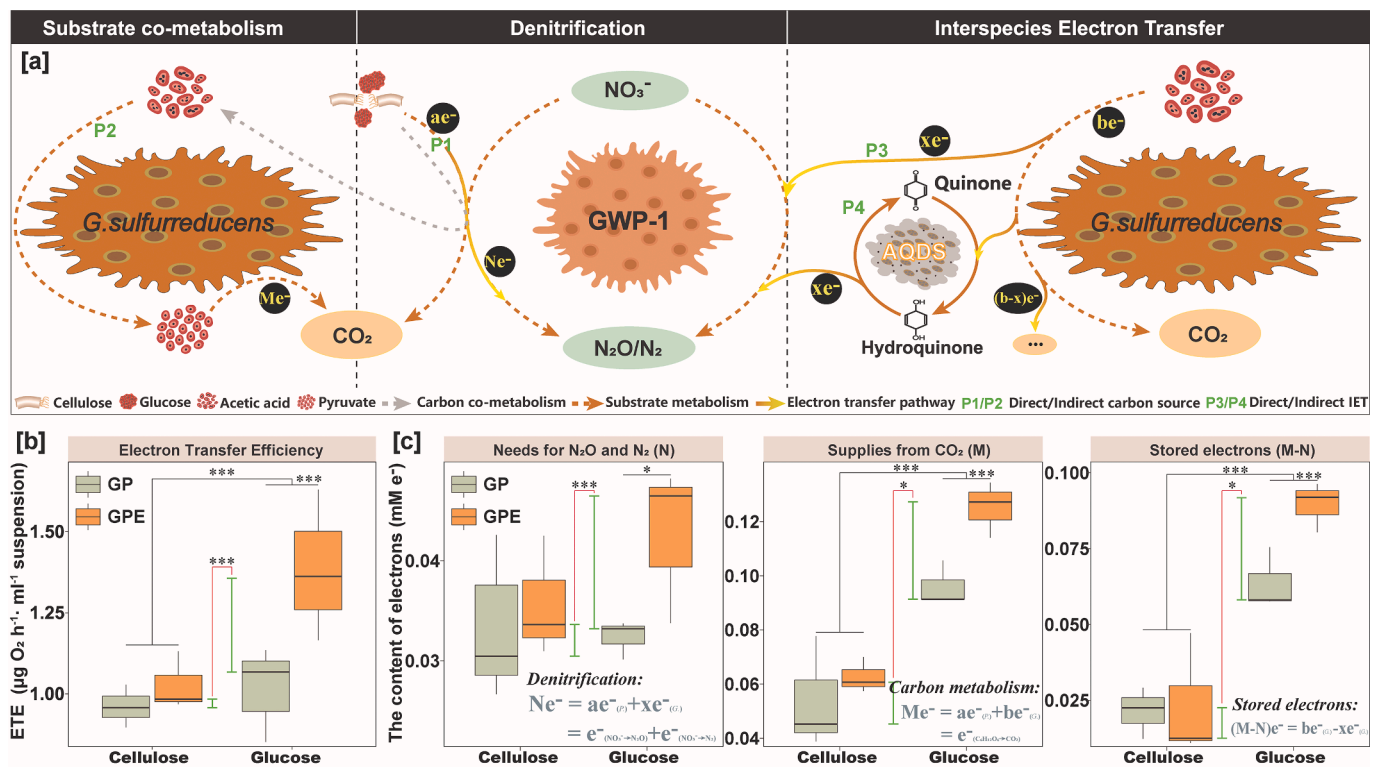
**Fig. 4.** **[a]** Syntrophy schematic model of *G. sulfurreduens* and GWP-1 mediated by substrate co-metabolism and interspecies electron transfer to drive the denitrification in co-culture system. **[b]** Electron transfers efficiency of *G. sulfurreduens* and GWP-1 in co-culture system feeding with glucose and cellulose in the presence/absence of AQDS. **[c]** Quantity of electrons for the denitrifying requirements, carbon consumption, AQDS store, and interspecies transfer were quantified in co-culture systems fed with glucose and cellulose in the presence/absence of AQDS (M, N, and M−N) and different carbon source groups (*x*). The differences in different groups were analyzed, and the green distance lines are value gaps between with/without AQDS for the values of N, M, and M−N in [c]. Asterisks (*) indicate significant differences (n = 3, $P < 0.05$). (For interpretation of the references to colour in this figure legend, the reader is referred to the web version of this article.)

with common gram-negative denitrifying bacteria, achieving interspecies electron syntrophy through direct electron transfer; on the other hand, it showed that with the addition of electron mediators, recalcitrant organic compounds can be efficiently degraded, driving effective nitrate reduction from the low-carbon effluent of WWTPs.

Although some studies showed that EAB can enhance denitrifying bacteria activity (Wan et al., 2018; Guo et al., 2023), the direct IET process between EAB has not been proven. In this study, we observed the formation of *G. sulfurreducens* and GWP-1 aggregates and the presence of filamentary cable (named as "nanowire") (Jiang et al., 2018; Boesen et al., 2021) between them, which seemly demonstrated the presence of direct IET between *G. sulfurreducens* and GWP-1 (Walker et al., 2020). Besides, we demonstrated that AQDS (mediator) not only improved the metabolic activity of *G. sulfurreducens* but also enhanced their electron export efficiency. In our study, carbon sources were theoretically sufficient in the experiment system. After small molecular organic matter from cellulose or glucose biodegradation being utilized by *G. sulfurreducens* through extracellular electron transport chains, a significant potential difference existed between *G. sulfurreducens*, oxidized AQDS, and GWP-1. This potential difference facilitated the directional transfer of electrons. AQDS stored the electrons after accepting them, and GWP-1 subsequently used these electrons to reduce nitrate. The carbon sources were cellulose and glucose, both of which can be metabolized by GWP-1. Moreover, the small-molecule carbon metabolites derived from these carbon sources could be further utilized by *G. sulfurreducens*. As a result, the electrons generated by *G. sulfurreducens* from metabolizing the carbon source were not directly transferred to GWP-1 (due to the absence of a significant potential difference between them). Instead, the electrons were stored in the quinone functional groups of AQDS, reducing them to hydroquinone (Fig. 3a). When GWP-1 could no longer obtain sufficient electrons from the cellulose carbon

source, a significant potential difference developed between AQDS and *G. sulfurreducens* on one side and GWP-1 on the other. This facilitated electron transfer and resulted in enhanced nitrate and nitrite reduction efficiency during this period (80 – 100 h, Fig. 2a).

Beyond observing direct and indirect IET between GWP-1 and *G. sulfurreducens*, this study quantified the IET via isotopic approach. The *G. sulfurreducens* supplied 0.071 mM electrons to GWP-1 when fed with cellulose, which decreased to 0.012 mM when fed with glucose. In other words, more electrons were provided by EAB when denitrifiers utilized a refractory carbon source, proving that EAB could favor denitrification even when small-molecular carbon sources are not available. These results could be explained through the combined analysis of electron transfer quantification and proteomics results. On one hand, cellulose, a recalcitrant carbon source, was degraded by extracellular cellulase from GWP-1 into small-molecule carbon sources, which could then be utilized by *G. sulfurreducens*. Through extracellular respiration, *G. sulfurreducens* transferred electrons to AQDS, facilitating an indirect IET process mediated by the electron mediator. On the other hand, glucose, a readily utilizable carbon source, could be efficiently metabolized by GWP-1. Under conditions with sufficient glucose, GWP-1 used it as an electron donor to reduce nitrate, thereby reducing the need for electrons supplied by other donors (Fig. 4b).

This makes it very promising to be applied in wastewater treatment, which could solve the problems of refractory carbon discharge and nitrogen discharge due to the lack of denitrification (Desmond-Le Quemener et al., 2021). Moreover, the isotopic approach is more advanced than previously applied chronoamperometry (Yuan et al., 2011) (measuring electron transfer capacity of mediators) or surface-enhanced Raman spectroscopy (Ly et al., 2013) (determining electron releasing rated from EAB), both of which cannot determine the number of electrons used for substance reduction or the effective electron transfer
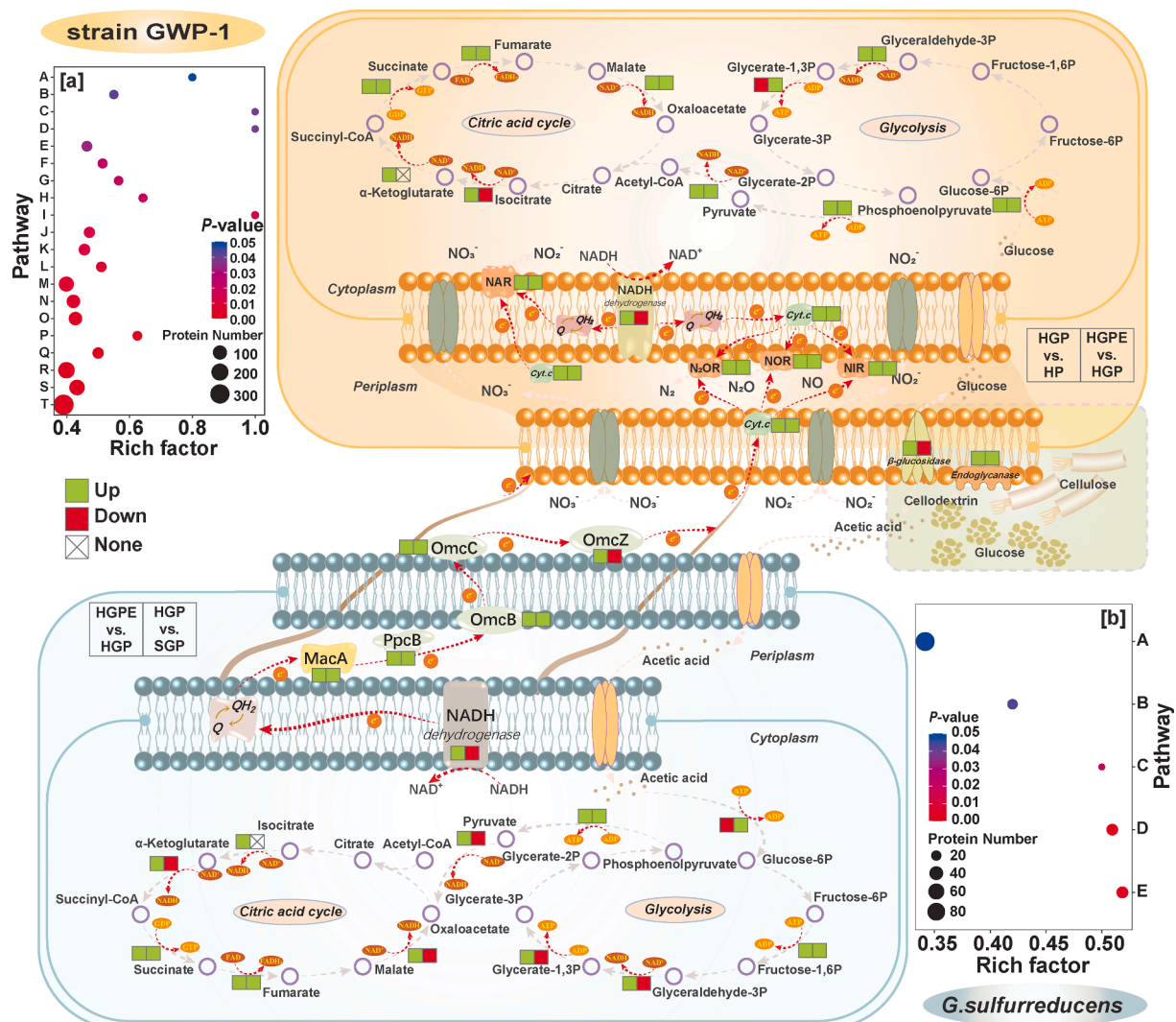
**Fig. 5.** Metabolic model of *G. sulfurreduens* and GWP-1 was focused by the proteome analysis. Colors indicate that the relative abundance of functional proteins was up (green) or down (red) in the different groups or the proteins were not annotated in the database (cross). **[a]** and **[b]** are the statistical graphs of significantly enriched pathways for GWP-1 in HGPE vs. SGPE and *G. sulfurreducens* in HGPE vs. HGP, respectively. A higher value indicates a larger proportion of differentially expressed proteins. The size of the dots in the Fig. represents the number of differentially expressed proteins annotated to that pathway (A, B, …, and specific process names are provided in the supplementary materials, Table S2). (For interpretation of the references to colour in this figure legend, the reader is referred to the web version of this article.)

amount.

Regardless of carbon sources, glucose and cellulose, as carbon sources, only were utilized by GWP-1, while *G. sulfurreducens* cannot utilize either of these carbon sources. Therefore, carbon source competition didn't occur in this study. We observed significantly increase of denitrification efficiency and decrease of $N_2O$ emission by co-culturing GWP-1 and *G. sulfurreducens*. For example, when using cellulose, the co-culture system increased the denitrification efficiency by 15.0 %, which was further enhanced by an additional 21.3 % after adding AQDS. Those results indicated that there is no competition for both of two carbon sources. At the same time, the co-culture system achieved 36.3 % (with AQDS) and 18.5 % (without AQDS) reduction in $N_2O$ emission ($CO_{2\text{-eq}}$) compared to that of a pure culture system. This is remarkable, considering the needs and difficulties in wastewater treatment regarding deep carbon and nitrate removal. Meanwhile, it paves a new route for wastewater treatment that can enhance denitrification using the left-over refractory carbon instead of adding additional small molecule carbon (e.g. glucose or acetate).

In the co-culture system with AQDS, the enhanced denitrification, cellulose utilization and $N_2O$ reduction were achieved through

synergistic interaction between *G. sulfurreducens* and GWP-1 and the increase of key genes and enzymatic proteins (Zhai et al., 2022; Tang et al., 2024), involving direct and indirect IET and the co-metabolism processes. However, this did not occur until 100 h, after sufficient proliferation of *G. sulfurreducens* and reduction of AQDS quinone groups. The mechanisms might be different for different carbon sources: i) only IET when glucose is the carbon source; ii) substrate co-metabolism and IET processes when cellulose is the carbon source. Evidenced by proteomic analysis, we observed key enzymes (e.g. endoglycanase and β-glucosidase) being responsible for the production of small molecular carbon sources generated from glucose and cellulose degradation by GWP-1 were utilized by *G. sulfurreducens* (known as "cross-feeding" (D'Souza et al., 2018), which aided GWP-1 in successfully completing denitrification and reducing $N_2O$ production. Through proteomics analysis and electron transfer quantification, we have also demonstrated that AQDS not only improves the metabolic activity of *G. sulfurreducens* but also enhances their electron export efficiency.

In summary, we pioneered the use of isotope tracing to quantitatively measure effective electron transfer amount to reduce the nitrate in the presence or absence of electron mediators and under feeding

different carbon source. This study extends prior knowledge by revealing the enhanced IET process and critical co-metabolic patterns involved in electron acceptor reduction and residual carbon source degradation. We demonstrated that the co-culture of EAB and denitrifiers not only enhanced refractory carbon degradation and deep denitrification, but also reduced N$_2$O emission during wastewater treatment. It is evident that AQDS was used at a very low concentration of just 100 μg/L in this study, yet it played a significant role. As a representative humic substance material, AQDS can be replaced with humic substances with similar functions in engineering applications. Moreover, its charge–discharge cycling ensures its potential for long-term effectiveness in wastewater treatment systems. From this perspective, AQDS and similar auxiliary enhancement materials offer a unique economic advantage in improving denitrification performance in wastewater treatment systems. It is important to acknowledge that this study is grounded in bacterial culture experiments and may not fully capture the complexity of actual environmental conditions. Nonetheless, our findings provide a robust theoretical basis and practical guidelines for advancing denitrification in real-world engineering systems.

## 5. Conclusion

In this study, we proved that the mutual symbiosis between EAB and denitrifiers could help solve residual carbon and nitrogen issues in wastewater treatment. The co-culture system of *G. sulfurreducens* and GWP-1 achieved a 3–5 time increase in refractory carbon degradation, a 40 % improvement in denitrification, and a 36 % reduction in N$_2$O emissions. This enhancement was driven by IET and carbon co-metabolism processes, quantified using isotopic tracing, which showed *G. sulfurreducens* supplying more electrons when cellulose was used as the carbon source. The findings suggest a synergistic approach for nitrogen pollution control and carbon reduction in wastewater treatment.

## CRediT authorship contribution statement

**Xiangyu Yang:** Writing – review & editing, Writing – original draft, Visualization, Validation, Supervision, Software, Resources, Project administration, Methodology, Investigation, Funding acquisition, Formal analysis, Data curation, Conceptualization. **Mingchen Yao:** Writing – review & editing, Visualization, Validation, Methodology, Investigation, Formal analysis, Data curation. **Peng Li:** Writing – review & editing, Supervision. **Jan Peter van der Hoek:** Investigation. **Lujing Zhang:** Writing – review & editing, Supervision. **Gang Liu:** Writing – review & editing, Supervision, Methodology, Investigation, Formal analysis, Data curation, Conceptualization.

## Declaration of competing interest

The authors declare that they have no known competing financial interests or personal relationships that could have appeared to influence the work reported in this paper.

## Appendix A. Supplementary material

Supplementary data to this article can be found online at https://doi.org/10.1016/j.envint.2025.109330.

## Data availability

Data will be made available on request.

## References

Aguirre-Sierra, A., Bacchetti-De Gregoris, T., Jose Salas, J., de Deus, A., Esteve-Nunez, A., 2020. A new concept in constructed wetlands: assessment of aerobic electroconductive biofilters. *Environ. Sci.-Water Res. Technol.* 6 (5), 1312–1323.

Boesen, T., Nielsen, L.P., Schramm, A., 2021. Pili for nanowires. *Nat. Microbiol.* 6 (11), 1347–1348.

Broberg, A., 1985. A modified method for studies of electron-transport system activity in fresh-water sediments. *Hydrobiologia* 120 (2), 181–187.

Buzzini, A.P., Miwa, D.W., Motheo, A.J., Pires, E.C., 2006. Use of electrochemical oxidation process as post-treatment for the effluents of a UASB reactor treating cellulose pulp mill wastewater. *Water Sci. Technol.* 54 (2), 207–213.

Climate Change, 2022. Mitigation of Climate Change: Working Group III Contribution to the Sixth Assessment Report of the Intergovernmental Panel on Climate Change. Cambridge University Press: Cambridge, 2023.

Chen, Y., Wen, Y., Tang, Z.R., Huang, J.G., Zhou, Q., Vymazal, J., 2015. Effects of plant biomass on bacterial community structure in constructed wetlands used for tertiary wastewater treatment. *Ecol. Eng.* 84, 38–45.

Desmond-Le Quemener, E., Moscoviz, R., Bernet, N., Marcus, A., 2021. Modeling of interspecies electron transfer in anaerobic microbial communities. *Curr. Opin. Biotechnol.* 67, 49–57.

Doherty, L., Zhao, Y., Zhao, X., Hu, Y., Hao, X., Xu, L., Liu, R., 2015. A review of a recently emerged technology: constructed wetland - microbial fuel cells. *Water Res.* 85, 38–45.

D'Souza, G., Shitut, S., Preussger, D., Yousif, G., Waschina, S., Kost, C., 2018. Ecology and evolution of metabolic cross-feeding interactions in bacteria. *Nat. Prod. Rep.* 35 (5), 455–488.

Du, W.-J., Lu, J.-Y., Hu, Y.-R., Xiao, J., Yang, C., Wu, J., Huang, B., Cui, S., Wang, Y., Li, W.-W., 2023. Spatiotemporal pattern of greenhouse gas emissions in China's wastewater sector and pathways towards carbon neutrality. *Nat. Water* 1 (2), 166–175.

Garrido-Amador, P., Stortenbeker, N., Wessels, H.J.C.T., Speth, D.R., Garcia-Heredia, I., Kartal, B., 2023. Enrichment and characterization of a nitric oxide-reducing microbial community in a continuous bioreactor. *Nat. Microbiol.* 8 (8), 1574–1586.

Graf, J.S., Schorn, S., Kitzinger, K., Ahmerkamp, S., Woehle, C., Huettel, B., Schubert, C. J., Kuypers, M.M.M., Milucka, J., 2021. Anaerobic endosymbiont generates energy for ciliate host by denitrification. *Nature* 591 (7850), 445–450.

Guo, F., Luo, Y., Nie, W., Xiong, Z., Yang, X., Yan, J., Liu, T., Chen, M., Chen, Y., 2023. Biochar boosts nitrate removal in constructed wetlands for secondary effluent treatment: Linking nitrate removal to the metabolic pathway of denitrification and biochar properties. *Bioresour. Technol.* 129000.

Guo, W., Ying, X., Zhao, N., Yu, S., Zhang, X., Feng, H., Zhang, Y., Yu, H., 2023. Interspecies electron transfer between *Geobacter* and denitrifying bacteria for nitrogen removal in bioelectrochemical system. *Chem. Eng. J.* 455, 139821.

Huang, M.-Q., Cui, Y.W., Huang, J.-L., Sun, F.-L., Chen, S., 2022. A novel Pseudomonas aeruginosa strain performs simultaneous heterotrophic nitrification-aerobic denitrification and aerobic phosphate removal. *Water Res.* 221, 118823.

Jiang, Z., Zhang, S., Klausen, L.H., Song, J., Li, Q., Wang, Z., Stokke, B.T., Huang, Y., Besenbacher, F., Nielsen, L.P., Dong, M., 2018. In vitro single-cell dissection revealing the interior structure of cable bacteria. *PNAS* 115 (34), 8517–8522.

Jones, E.R., van Vliet, M.T.H., Qadir, M., Bierkens, M.F.P., 2021. Country-level and gridded estimates of wastewater production, collection, treatment and reuse. *Earth Syst. Sci. Data* 13 (2), 237–254.

Kato, S., Hashimoto, K., Watanabe, K., 2012. Microbial interspecies electron transfer via electric currents through conductive minerals. *PNAS* 109 (25), 10042–10046.

Kato, S., Hashimoto, K., Watanabe, K., 2012. Methanogenesis facilitated by electric syntrophy via (semi)conductive iron-oxide minerals. *Environ. Microbiol.* 14 (7), 1646–1654.

Liu, Y., Ding, M., Ling, W., Yang, Y., Zhou, X., Li, B.-Z., Chen, T., Nie, Y., Wang, M., Zeng, B., Li, X., Liu, H., Sun, B., Xu, H., Zhang, J., Jiao, Y., Hou, Y., Yang, H., Xiao, S., Lin, Q., He, X., Liao, W., Jin, Z., Xie, Y., Zhang, B., Li, T., Lu, X., Li, J., Zhang, F., Wu, X.-L., Song, H., Yuan, Y.-J., 2017. A three-species microbial consortium for power generation. *Energ. Environ. Sci.* 10 (7), 1600–1609.

Liu, F., Rotaru, A.-E., Shrestha, P.M., Malvankar, N.S., Nevin, K.P., Lovley, D.R., 2012. Promoting direct interspecies electron transfer with activated carbon. *Energ. Environ. Sci.* 5 (10), 8982–8989.

Liu, X., Yang, X., Hu, X., He, Q., Zhai, J., Chen, Y., Xiong, Q., Vymazal, J., 2019. Comprehensive metagenomic analysis reveals the effects of silver nanoparticles on nitrogen transformation in constructed wetlands. *Chem. Eng. J.*, 358, 1552–1560.

Livak, K.J., Schmittgen, T.D., 2001. Analysis of relative gene expression data using real-time quantitative PCR and the 2(T)(-Delta Delta C) method. *Methods* 25 (4), 402–408.

Lu, L., Xing, D., Ren, Z.J., 2015. Microbial community structure accompanied with electricity production in a constructed wetland plant microbial fuel cell. *Bioresour. Technol.* 195, 115–121.

Ly, H.K., Harnisch, F., Hong, S.-F., Schroeder, U., Hildebrandt, P., Millo, D., 2013. Unraveling the interfacial electron transfer dynamics of electroactive microbial biofilms using surface-enhanced raman spectroscopy. *ChemSusChem* 6 (3), 487–492.

Ma, J., Chen, T., Wu, S., Yang, C., Bai, M., Shu, K., Li, K., Zhang, G., Jin, Z., He, F., Hermjakob, H., Zhu, Y., 2019. iProX: an integrated proteome resource. *Nucleic Acids Res.* 47 (D1), D1211–D1217.

Ma, J., Liu, M.T., Wang, Y.C., Xin, C., Zhang, H., Chen, S.R., Zheng, X.D., Zhang, X.J., Xiao, F.L., Yang, S., 2020. Quantitative proteomics analysis of young and elderly skin with DIA mass spectrometry reveals new skin aging-related proteins. *Aging-Us* 12 (13), 13529–13554.

Morita, M., Malvankar, N.S., Franks, A.E., Summers, Z.M., Giloteaux, L., Rotaru, A.E., Rotaru, C., Lovley, D.R., 2011. Potential for direct interspecies electron transfer in methanogenic wastewater digester aggregates. *MBio* 2 (4).

Niemann, H.B., Atreya, S.K., Bauer, S.J., Carignan, G.R., Demick, J.E., Frost, R.L., Gautier, D., Haberman, J.A., Harpold, D.N., Hunten, D.M., Israel, G., Lunine, J.I., Kasprzak, W.T., Owen, T.C., Paulkovich, M., Raulin, F., Raaen, E., Way, S.H., 2005. The abundances of constituents of Titan's atmosphere from the GCMS instrument on the Huygens probe. *Nature* 438 (7069), 779–784.

Roots, P., Wang, Y., Rosenthal, A.F., Griffin, J.S., Sabba, F., Petrovich, M., Yang, F., Kozak, J.A., Zhang, H., Wells, G.F., 2019. Comammox Nitrospira are the dominant ammonia oxidizers in a mainstream low dissolved oxygen nitrification reactor. *Water Res* 157, 396–405.

Rothausen, S.G.S.A., Conway, D., 2011. Greenhouse-gas emissions from energy use in the water sector. *Nat. Clim. Chang.* 1 (4), 210–219.

Scott, D.T., McKnight, D.M., Blunt-Harris, E.L., Kolesar, S.E., Lovley, D.R., 1998. Quinone moieties act as electron acceptors in the reduction of humic substances by humics-reducing microorganisms. *Environ. Sci. Tech.* 32 (19), 2984–2989.

Shi, L., Dong, H., Reguera, G., Beyenal, H., Lu, A., Liu, J., Yu, H.-Q., Fredrickson, J.K., 2016. Extracellular electron transfer mechanisms between microorganisms and minerals. *Nat. Rev. Microbiol.* 14 (10), 651–662.

Su, X., Wen, T., Wang, Y., Xu, J., Cui, L., Zhang, J., Xue, X., Ding, K., Tang, Y., Zhu, Y.-G., 2021. Stimulation of N$_2$O emission via bacterial denitrification driven by acidification in estuarine sediments. *Glob. Chang. Biol.* 27 (21), 5564–5579.

Summers, Z.M., Fogarty, H.E., Leang, C., Franks, A.E., Malvankar, N.S., Lovley, D.R., 2010. Direct exchange of electrons within aggregates of an evolved syntrophic coculture of anaerobic bacteria. *Science* 330 (6009), 1413–1415.

Tang, M., Ma, S., Yao, S., Lu, F., Yang, Y., 2024. Enhanced denitrification performance and extracellular electron transfer for eletrotrophic bio-cathode mediated by anthraquinone-2, 6-disulfonate (AQDS) at low temperature. *Int. J. Hydrogen Energy* 84, 215–223.

van der Hoek, J.P., de Fooij, H., Struker, A., 2016. Wastewater as a resource: strategies to recover resources from Amsterdam's wastewater. *Resour. Conserv. Recycl.* 113, 53–64.

Walker, D.J.F., Nevin, K.P., Holmes, D.E., Rotaru, A.-E., Ward, J.E., Woodard, T.L., Zhu, J., Ueki, T., Nonnenmann, S.S., McInerney, M.J., Lovley, D.R., 2020. *Syntrophus* conductive pili demonstrate that common hydrogen-donating syntrophs can have a direct electron transfer option. *ISME J.* 14 (3), 837–846.

Wan, Y., Zhou, L., Wang, S., Liao, C., Li, N., Liu, W., Wang, X., 2018. Syntrophic growth of geobacter sulfurreducens accelerates anaerobic denitrification. *Front. Microbiol.* 9, 1572.

Wang, Q., He, J., 2020. Complete nitrogen removal via simultaneous nitrification and denitrification by a novel phosphate accumulating Thauera sp. strain SND5. *Water Res.* 185.

Wastewater monitoring comes of age, 2022. Nat. Microbiol., 7(8), 1101-1102.

Xu, M., Deng, J.W., Xu, K.K., Zhu, T.S., Han, L., Yan, Y.H., Yao, D.N., Deng, H., Wang, D., Sun, Y.T., Chang, C., Zhang, X.M., Dai, J.Y., Yue, L., Zhang, Q.S., Cai, X., Zhu, Y., Duan, H., Liu, Y., Li, D., Zhu, Y.P., Radstake, T., Balak, D.M.W., Xu, D.K., Guo, T.N., Lu, C.J., Yu, X.B., 2019. In-depth serum proteomics reveals biomarkers of psoriasis severity and response to traditional Chinese medicine. *Theranostics* 9 (9), 2475–2488.

Yan, J., Hu, X., He, Q., Qin, H., Yi, D., Lv, D., Cheng, C., Zhao, Y., Chen, Y., 2021. Simultaneous enhancement of treatment performance and energy recovery using pyrite as anodic filling material in constructed wetland coupled with microbial fuel cells. *Water Res.* 201, 117333.

Yang, X., He, Q., Guo, F., Sun, X., Zhang, J., Chen, M., Vymazal, J., Chen, Y., 2020. Nanoplastics disturb nitrogen removal in constructed wetlands: responses of microbes and macrophytes. *Environ. Sci. Tech.* 54 (21), 14007–14016.

Yang, X., Zhang, L., Chen, Y., He, Q., Liu, T., Zhang, G., Yuan, L., Peng, H., Wang, H., Ju, F., 2022. Micro(nano)plastic size and concentration co-differentiate nitrogen transformation, microbiota dynamics, and assembly patterns in constructed wetlands. *Water Res.* 220, 118636.

Yao, M.C., Zhang, Y., Dai, Z.H., Ren, A.R., Fang, J.X., Li, X.M., van der Meer, W., Medema, G., Rose, J.B., Liu, G., 2023. Building water quality deterioration during water supply restoration after interruption: Influences of premise plumbing configuration. *Water Res.* 241, 120149.

Yuan, T., Yuan, Y., Zhou, S., Li, F., Liu, Z., Zhuang, L., 2011. A rapid and simple electrochemical method for evaluating the electron transfer capacities of dissolved organic matter. *J. Soil. Sediment.* 11 (3), 467–473.

Zhai, S., Cheng, H., Wang, Q., Zhao, Y., Wang, A., Ji, M., 2022. Reinforcement of denitrification in a biofilm electrode reactor with immobilized polypyrrole/anthraquinone-2,6-disulfonate composite cathode. *J. Environ. Manage.* 315.

Zhou, Q., Sun, H., Jia, L., Wu, W., Wang, J., 2022. Simultaneous biological removal of nitrogen and phosphorus from secondary effluent of wastewater treatment plants by advanced treatment: A review. *Chemosphere* 296.

Zhu, T.S., Zhu, Y., Xuan, Y., Gao, H.H., Cai, X., Piersma, S.R., Pham, T.V., Schelfhorst, T., Haas, R., Bijnsdorp, I.V., Sun, R., Yue, L., Ruan, G., Zhang, Q.S., Hu, M., Zhou, Y., Van Houdt, W.J., Le Large, T.Y.S., Cloos, J., Wojtuszkiewicz, A., Koppers-Lalic, D., Bottger, F., Scheepbouwer, C., Brakenhoff, R.H., van Leenders, G., Ijzermans, J.N.M., Martens, J.W.M., Steenbergen, R.D.M., Grieken, N.C., Selvarajan, S., Mantoo, S., Lee, S.S., Yeow, S.J.Y., Alkaff, S.M.F., Xiang, N., Sun, Y.T., Yi, X., Dai, S.Z., Liu, W., Lu, T., Wu, Z.C., Liang, X., Wang, M., Shao, Y.K., Zheng, X., Xu, K.L., Yang, Q., Meng, Y.F., Lu, C., Zhu, J., Zheng, J.E., Wang, B., Lou, S., Dai, Y.B., Xu, C., Yu, C.H., Ying, H.Z., Lim, T.K., Wu, J.M., Gao, X.F., Luan, Z.Z., Teng, X.D., Wu, P., Huang, S. A., Tao, Z.H., Iyer, N.G., Zhou, S.G., Shao, W.G., Lam, H., Ma, D., Ji, J.F., Kon, O.L., Zheng, S., Aebersold, R., Jimenez, C.R., Guo, T.N., 2020. DPHL: A DIA pan-human protein mass spectrometry library for robust biomarker discovery. *Genom. Proteomics Bioinformat.* 18 (2), 104–119.